SPANDIDOS PUBLICATIONS

ONCOLOGY LETTERS 16: 3439-3446, 2018

In vivo acquired sorafenib-resistant patient-derived tumor model displays alternative angiogenic pathways, multi-drug resistance and chromosome instability

GANG HU[1-4*], YIXIN ZHANG[5*], KEDONG OUYANG[2], FUBO XIE[2,3], HOUSHUN FANG[2], XUEYANG YANG[2], KUNYAN LIU[2-4], ZONGYU WANG[2,3], XUZHEN TANG[2], JIBIN LIU[5], LEI YANG[5], ZHENZHOU JIANG[1], WEIKANG TAO[2,6], HE ZHOU[2,3] and LUYONG ZHANG[1]

[1]Jiangsu Key Laboratory of Drug Screening, China Pharmaceutical University, Nanjing, Jiangsu 210009; [2]Shanghai ChemPartner Co., Ltd.; [3]Shanghai Engineering Research Center of Pharmaceutical Translation; [4]ClinicalExplorer (Shanghai) Co., Ltd., Shanghai 201203; [5]Department of Surgery, Nantong Cancer Hospital, Nantong, Jiangsu 226361, P.R. China

Received October 14, 2016; Accepted September 28, 2017

DOI: 10.3892/ol.2018.9078

Abstract. Acquired resistance to targeted therapies is an important clinical challenge. Research focusing on acquired resistance is hindered by the lack of relevant model systems. In the present study, the generation and characterization of an *in vivo* acquired sorafenib-resistant hepatocellular carcinoma (HCC) xenograft model derived from a patient tumor is reported. A cancer cell line (LIXC-004SR) was generated from a tumor that had developed following ~100 days of sorafenib treatment of a HCC patient-derived xenograft (PDX) model (LIX004). The xenograft tumors derived from this cell line demonstrated sorafenib-resistance *in vivo*. By contrast, a cell line (LIXC-004NA) generated from a vehicle-treated LIX004 PDX model remained sensitive to sorafenib *in vivo*. Following treatment with sorafenib *in vivo*, angiogenesis was significantly elevated in the LIXC-004SR tumors when compared with that in the LIXC-004NA tumors. The LIXC-004SR cell culture supernatant stimulated human umbilical vein endothelial cell proliferation and extracellular-signal-regulated kinase and protein kinase B phosphorylation, which can only be inhibited by the combination of sorafenib and a fibroblast growth factor receptor 1 (FGFR1) inhibitor, AZD4547. The tumor growth of the sorafenib-resistant LIXC-004SR xenograft was inhibited by the FGFR1 inhibitor *in vivo*, suggesting that one of the underlying mechanisms of the acquired resistance is likely due to activation of alternative angiogenic pathways. The LIXC-004SR cell line also exhibited signs of multi-drug resistance and genetic instability. Taken together, these data suggest that this *in vivo* model of acquired resistance from a PDX model may reflect sorafenib-resistance in certain patients and may facilitate drug resistance research, as well as contributing to the clinical prevention and management of drug resistance.

Correspondence to: Dr He Zhou, Shanghai ChemPartner Co., Ltd., Room 202, Building 6, 998 Halei Road, Shanghai 201203, P.R. China
E-mail: zhhe@chemparnter.cn

Dr Luyong Zhang, Jiangsu Key Laboratory of Drug Screening, China Pharmaceutical University, 24 Tongjia Xiang, Nanjing, Jiangsu 210009, P.R. China
E-mail: lyonzhang@163.com

Present address: [6]Shanghai Hengrui Medicine Co., Ltd., Shanghai 200245, P.R. China

[*]Contributed equally

Abbreviations: HCC, hepatocellular carcinoma; PDX, patient-derived xenograft; HUVECs, human umbilical vein endothelial cells

Key words: acquired resistance, hepatocellular carcinoma, patient-derived xenograft, sorafenib, fibroblast growth factor

Introduction

Liver cancer is responsible for the second highest number of cancer-associated fatalities in men worldwide, following lung cancer. Hepatocellular carcinoma (HCC) accounts for 70-85% of all liver cancer types (1). Sorafenib is a multi-kinase inhibitor that inhibits angiogenesis and tumor cell proliferation (2). Sorafenib treatment has demonstrated survival benefits and good tolerability in clinical trials (3), and has become the standard treatment option for advanced HCC. Despite its success, sorafenib treatment extended patient overall survival by only 2-3 months in previous studies (3,4). Even among those who initially responded well to sorafenib treatment, the majority of patients developed drug resistance during treatment (3,5). Currently, there is no effective systemic therapy available for patients following failure of sorafenib therapy (6,7). Therefore, preventing or treating sorafenib resistance has become an urgent unmet medical requirement.

Acquired drug resistance develops in the context of tumor-host interactions. In order to understand the key

mechanisms of sorafenib resistance, one such model was developed from an HCC patient-derived xenograft (PDX) model following long-term sorafenib-treatment. A PDX model was selected as these models preserve numerous clinical characteristics and their drug response is markedly associated with clinical drug efficacy (8-10). To facilitate mechanistic studies, cell lines were established from the vehicle-treated and sorafenib-treated xenografts. Through comparing the two cell lines and respective xenografts, the present study demonstrated that the *in vivo* sorafenib resistance of the LIXC-004SR cell line appears to be partially mediated by alternative angiogenesis pathways.

Materials and methods

Patient samples. Surgically removed human HCC samples were obtained from Nantong Cancer Hospital (Nantong, Jiangsu, China) and written informed consent was obtained according to protocols approved by the ChemPartner Institutional Ethical Committee.

Animals. A total of 5 female 6-8-week-old severe combined immune deficiency (SCID) mice and ~150 female 6-8-week-old Nu/Nu mice (16-20 g) were purchased from Beijing Vital River Laboratory Animal Technology Co. Ltd. (Beijing, China) and used for different experiments, including the PDX model establishment, sorafenib resistant model generation, tumorigenicity of cell lines, and *in vivo* efficacy study of these cell lines. Animals were housed under specific pathogen-free conditions at ChemPartner. Animals for at least three days for acclimation prior to the study. Animals were provided pelleted food and water *ad libitum* and kept in a room conditioned at 20-25˚C, 40-70% relative humidity with a 12 h light/dark cycle according to guidelines provided by the Association for Assessment and Accreditation of Laboratory Animal Care. The experiment was performed according to the protocol approved by the ChemPartner Institutional Animal Care and Use Committee.

Reagents. Sorafenib was purchased from LC Laboratories (Woburn, MA, USA) and AZD4547 [a selective inhibitor for fibroblast growth factor (FGF) receptor 1] was purchased from Shanghai Biochempartner Co., Ltd. (Shanghai, China). For *in vivo* studies, sorafenib was dissolved in cremophor (Sigma-Aldrich; Merck KGaA, Darmstadt, Germany), ethanol and distilled water (12.5:12.5:75, respectively), and administered orally each day at a dosage of 40 mg/kg (2,11). AZD4547 was dissolved in 1% Tween-80 (Sigma-Aldrich; Merck KGaA) in distilled water, sonicated for 30 min and mixed thoroughly and administered orally each day at a dosage of 12.5 mg/kg (dosage volume, 10 ml/kg) (12).

Establishment of cell lines from PDX. A PDX model, LIX004, was established by implantation of primary HCC tumor fragments from a 39-year-old female patient subcutaneously into the right flank of SCID mice with Matrigel (BD Biosciences, Franklin Lakes, NJ, USA) and subsequent passaging in Nu/Nu mice. The primary tumor cells isolated from a tumor obtained from vehicle-treated (10 ml/kg) or sorafenib-treated (40 mg/kg, orally once daily, for ~100 days) mice were used for HCC cell line establishment (Fig. 1) (13). All tissue culture media and supplements were purchased from Thermo Fisher Scientific, Inc. (Waltham, MA, USA). Tumor cells were suspended in serum-free medium and were incubated continuously in a 37˚C and 5% CO_2 incubator (Thermo Fisher Scientific, Inc.). Half of the medium was changed every 3-4 days and the cells were subcultured at 70-80% confluence. When the cancer cell lines grew stably, the culture medium was gradually changed to RPMI-1640 medium supplemented with 10% fetal bovine serum and10 μg/ml human insulin. Cultures were tested negative for *Mycoplasma* contamination using polymerase chain reaction analysis (MycoScan™ *Mycoplasma* Detection Kit; HD Biosciences, Shanghai, China), according to the manufacturer's protocol. Cells in the exponential growth phase were used in subsequent experiments following passage 20.

Cells. HUVECs were obtained from All Cells-Shanghai (Shanghai, China) and were used in studies within 7 passages.

Chromosome analysis. Metaphase cells were arrested using colchicines (Sigma-Aldrich; Merck KGaA) and fixed in methanol/acetic acid solution (3:1) prior to being stained with Giemsa solution (Thermo Fisher Scientific, Inc.) at room temperature for 20 min. The slides were mounted and the number of chromosomes was determined and observed using an Eclipse microscope (magnification, x1,000; Nikon Instruments Inc., Melville, NY, USA). The frequency was analyzed using Origin software (version 7.0; OriginLab, Northampton, MA, USA).

Short-tandem repeat (STR) assay. Cell line purity was verified by microsatellite/STR analysis. The genomic DNA was extracted and the STR amplicons were analyzed using an AmpF/STR® Identifiler® PCR Amplification kit (Thermo Fisher Scientific, Inc.) according to the manufacturer's protocols.

In vivo xenograft studies. In total, ~150 female Nu/Nu nude mice aged 6-8 weeks were used in various *in vivo* studies. Cultured tumor cells were subcutaneously injected into the right flank of the mice ($5.0x10^6$ cells/mouse) with 50% Matrigel. Animals with a tumor volume of 100-150 mm^3 (~60%) were selected and randomized for daily treatment with either the vehicle or sorafenib (n=8 or 10 per group). Un-enrolled animals (~40%) were euthanized with CO_2 anesthesia. Treated animals were monitored daily with tumor volume and body weight was recorded ≥2 times per week. If animals exhibited signs of distress, weight loss >20% of initial body weight and/or tumor volume >2,000 mm^3, they were sacrificed.

Immunohistochemical (IHC) analysis. Cells were cultured as a monolayer on sterile chamber slides prior to being fixed with 4% formaldehyde at 4˚C overnight. Tumor tissues were 4% formaldehyde-fixed at 4˚C for 48 h and paraffin-embedded and 5 μm slides were prepared. The slides were rehydrated in Xylene and a descending alcohol series. Antigen heat retrieval (at 100˚C) was performed in EDTA buffer (pH 9.0) or citrate buffer (pH 6.0, all from Fuzhou Maixin Biotech. Co., Ltd., Fuzhou, Fujian, China) and washed in running water and

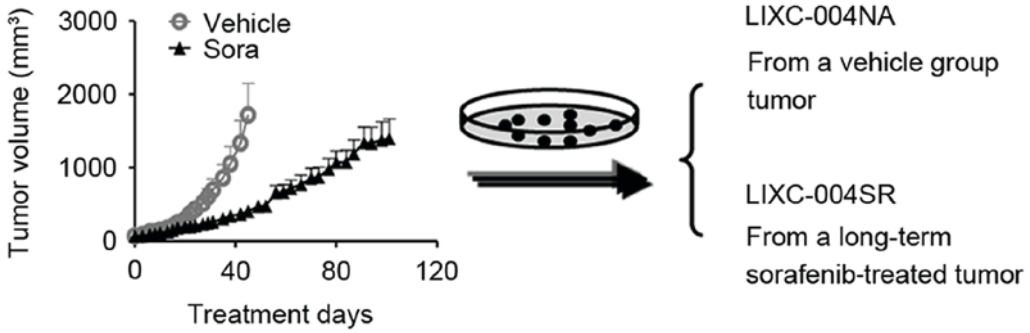

Figure 1. Schematic diagram of the establishment of the cell lines. A hepatocellular carcinoma PDX model LIX-004 was subjected to daily treatment with vehicle or sorafenib. Cell lines, LIXC-004NA (from a tumor of the vehicle-treated group) and LIXC-004SR (from a tumor developed following ~100 days of treatment with sorafenib), were established. PDX, patient-derived tumor xenograft; Sora, sorafenib.

then the IHC wash buffer (Fuzhou Maixin Biotech Co., Ltd.). The slides were blocked in 4% goat serum (Thermo Fisher Scientific, Inc.) in PBS at room temperature for 30 min, and then incubated with different primary antibodies at 4˚C overnight, including anti-cytokeratin antibody (cat no. 130-080-101; diluted at 1:50; Miltenyi Biotec GmbH, Bergisch, Gladbach, Germany), anti-α_1-fetoprotein (AFP) antibody (cat no. 7723-1; diluted at 1:200; Epitomics; Abcam, Cambridge, MA, USA), anti-vimentin antibody (cat no. 2707-1; diluted at 1:200; Epitomics; Abcam), and anti-CD34 antibody (cat no. 2150-1; diluted at 1:200; Epitomics; Abcam), which were diluted in the 4% goat serum blocking buffer. Slides were washed with the wash buffer and then incubated with secondary horseradish peroxidase-conjugated secondary antibody (cat no. K400311, Dako; Agilent Technologies, Inc., Santa Clara, CA, USA) at room temperature for 30 min, and then slides were developed using the 3,3'-diaminobenzidine method (Fuzhou Maixin Biotech, Co., Ltd) at room temperature for 4 min. Slides were then mounted and scanned using a ScanScope XT slide scanner (Aperio Group LLC, Sausalito, CA, USA) and $CD34^+$ areas were quantified using Image Scope software (vision 11.0, Aperio Group LLC).

Conditioned medium (CM) collection. LIXC-004NA or LIXC-004SR cells were seeded at a density of $2x10^6$ cells per 75-cm^2 flask. After 24 h, cells were washed twice with sterile PBS and medium was changed to serum-free medium (RPMI-1640) supplemented with 0.2% bovine serum albumin (purchased from Thermo Fisher Scientific, Inc.) and incubated at 37˚C for a further 48 h. Culture supernatant was collect and passed through a 0.45-μm filter.

HUVEC proliferation and western blot analysis. A HUVEC proliferation assay was performed with the cells inoculated into the poly-D-lysine-coated 96-well plates (BD Biosciences) and incubated at 37˚C overnight (2,000 cells/well). Culture medium was changed to 50% LIXC-004NA or LIXC-004SR CM and incubated at 37˚C for another 48 h. Cells were fixed in 4% formaldehyde at 4˚C overnight and treated with 0.1% Triton X-100 at room temperature for 10 min. Cell numbers were then quantified using Acumen eX3 (TTP Labtech Ltd., Melbourn, UK) following staining with 1.5 μM propidium iodide (Thermo Fisher Scientific, Inc.) at room temperature for 15 min in the dark.

HUVECs were seeded onto 6-well plates and incubated at 37˚C overnight, then serum-starved for 3 h, followed by compound treatment for 1 h prior to being stimulated with LIXC-004NA or LIXC-004SR CM for 10 min. Cells were washed with PBS twice, and western blot analysis was performed on the total protein.

Cell or tumor samples were lysed in cell lysis buffer (Cell Signaling Technology, Inc., Danvers, MA, USA) containing a Halt protease inhibitor (Thermo Fisher Scientific, Inc.) and a phosphatase inhibitor cocktail (Sigma-Aldrich; Merck KGaA). The protein concentration was determined using a bicinchoninic acid method (Beyotime Institute of Biotechnology, Haimen, China) and a total of 20 μg protein per sample was loaded onto NuPAGE™ 4-12% Bis-Tris Protein Gels. Proteins were transferred onto nitrocellulose membranes (all from Thermo Fisher Scientific, Inc.). Membranes were incubated with blocking buffer (LI-COR Biosciences, Lincoln, NE, USA) at room temperature for 1 h and incubated with primary antibodies at 4˚C overnight, including anti-extracellular-signal-regulated kinases (ERK) 1/2 antibody (cat no. 4695), phosphorylated (pho)-ERK1/2 (Thr202/Tyr204) antibody (cat no. 4370), protein kinase B (Akt) (cat no, 9272) antibody and pho-Akt (Ser437) antibody (Cat. No. 4060, all primary antibodies were diluted at 1:1,000, and purchased from Cell Signaling Technology, Inc.), followed by the Alexa Fluor 680-conjugated secondary antibody incubation (cat no. A21076; diluted at 1:10,000; Thermo Fisher Scientific, Inc.) at room temperature for 60 min. Blots were scanned using Odyssey systems (LI-COR Biosciences). Anti-GAPDH antibody (cat no. 5632-1; diluted at 1:2,000; Epitomics; Abcam) was used as a loading control.

Reverse transcription-quantitative polymerase chain reaction (RT-qPCR). Total RNA was extracted from each cell line using an RNeasy kit (Qiagen, Inc., Valencia, CA, USA) and complementary DNA (cDNA) was produced from 1 μg RNA using a RevertAid First Strand cDNA Synthesis kit (Thermo Fisher Scientific, Inc.). TaqMan primers for matrix metalloproteinase-1 (MMP-1; Hs00899658_m1), fibroblast growth factor 5 (FGF5; Hs00738132_m1), vascular endothelial growth factor A (VEGFA; Hs00899658_m1) and GAPDH (Hs02758991_g1) were used for RT-qPCR on a ViiA 7 System (Thermo Fisher Scientific, Inc.). All TaqMan primers were purchased from Thermo Fisher Scientific, Inc., and a TaqMan gene expression master mix kit (Thermo Fisher Scientific, Inc.) was used

according to the manufacturer's protocol. Each sample was assayed in duplicate and the ΔΔCq method was used to determine relative gene expression levels (14).

Statistical analysis. Data are presented as the mean ± standard deviation and the data of the *in vivo* efficacy studies are expressed as the mean ± standard error of the mean. Statistical differences between groups were analyzed using Student's t-test, one-way analysis of variance (ANOVA) or two-way ANOVA with Bonferroni post hoc test using Prism (version 5; GraphPad Software, La Jolla, CA, USA). $P<0.05$ was considered to indicate a statistically significant difference.

Results

LIXC-004SR cells are generated from sorafenib-treated HCC PDX tumors and exhibit signs of multi-drug resistance. To reproduce the acquired sorafenib resistance, Nu/Nu mice bearing LIX004 PDX tumors were treated with 40 mg/kg sorafenib daily. Despite retardation of tumor progression, the animals were not cured and, following ~100 days of sorafenib treatment, all animals developed tumors, with certain tumors reaching a volume of nearly 2,000 mm^3 (Fig. 1).

To determine the mechanisms of sorafenib resistance in the tumor, primary tumor cell lines were established. The cell line generated from the tumor, which had developed following long-term sorafenib treatment, was LIXC-004SR, and the cell line derived from a vehicle-treated tumor was LIXC-004NA (Fig. 1). LIXC-004SR cells exhibited a slightly shorter *in vitro* doubling time when compared with that of the LIXC-004NA cells (24.67 and 32.37 h, respectively). LIXC-004SR displayed less cytokeratin expression and each cell line expressed vimentin (Fig. 2A). STR analyses revealed that the two cell lines matched perfectly with the original PDX model (Fig. 2B) and thus that the two cell lines and the PDX had been derived from the same individual.

Furthermore, the two cell lines exhibited similar sensitivity to sorafenib, fluorouracil and docetexal, while LIXC-004SR displayed a decreased sensitivity to doxorubicin, vinblastine and erlotinib (Table I), despite the fact that the model had never been exposed to these drugs previously.

Sorafenib resistance of the LIXC-004SR xenograft in vivo. The two cell lines were tested for tumorigenicity *in vivo* and were able to produce xenograft tumors (Fig. 2C). When reviewed by a pathologist, the two xenografts were diagnosed as poorly differentiated HCC, as was the original PDX model (Fig. 2D).

When the average tumor size reached 100-150 mm^3, the tumor-bearing animals were randomized and treated with vehicle or 40 mg/kg sorafenib daily. The xenograft derived from the LIXC-004NA cell line responded to sorafenib treatment. Smaller, paler tumors were observed in the sorafenib-treated animals (Fig. 2C), suggesting that angiogenesis and tumor growth had been successfully inhibited. In contrast, when LIXC-004SR tumor-bearing animals were treated with sorafenib, 6/10 mice displayed tumors of a similar size when compared with those displayed by the vehicle group, while the other 4 animals developed tumors that were larger than any of those displayed by the vehicle control group (Fig. 2C), suggesting that the LIXC-004SR tumors were resistant to sorafenib in a number of the animals. The studies were repeated twice and similar tumor growth and drug response profiles were observed. Notably, the LIXC-004SR tumors grew faster than the LIXC-004NA tumors, using approximately half of the time to reach a tumor volume of ~1,500 mm^3 (Fig. 2C). In light of this, LIXC-004SR represents one of the few acquired sorafenib-resistant tumor models established from a PDX model.

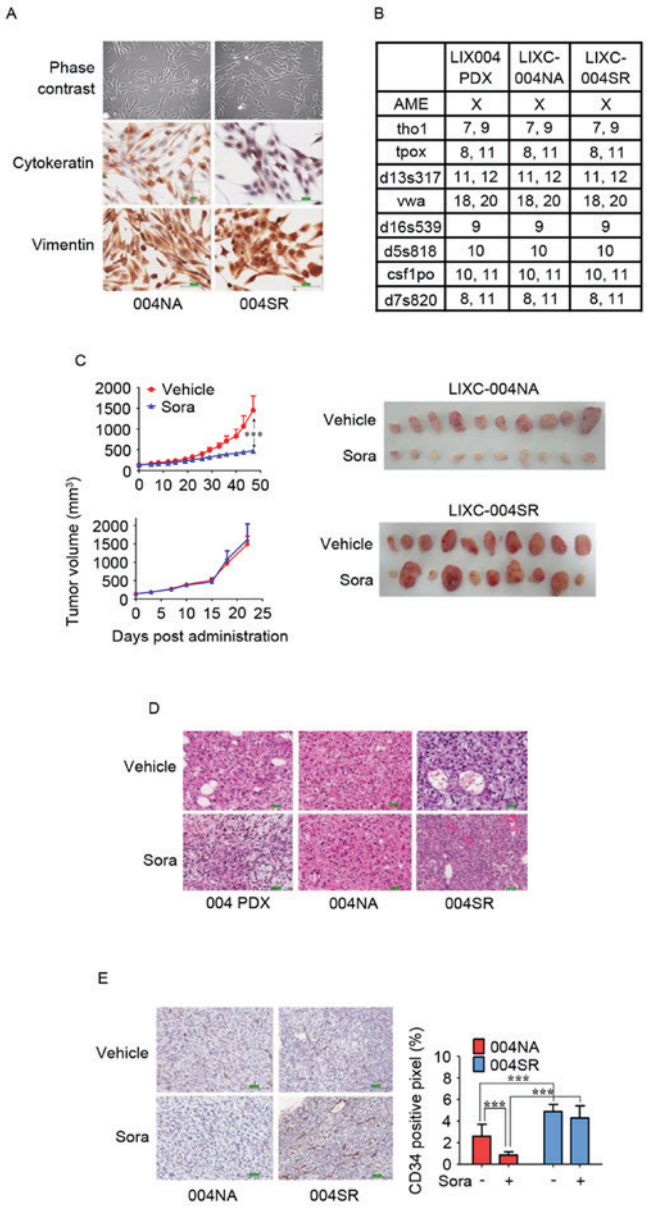

	LIX004 PDX	LIXC-004NA	LIXC-004SR
AME	X	X	X
tho1	7, 9	7, 9	7, 9
tpox	8, 11	8, 11	8, 11
d13s317	11, 12	11, 12	11, 12
vwa	18, 20	18, 20	18, 20
d16s539	9	9	9
d5s818	10	10	10
csf1po	10, 11	10, 11	10, 11
d7s820	8, 11	8, 11	8, 11

Figure 2. *In vitro* and *in vivo* characterization of LIXC-004NA and LIXC-004SR cell lines. (A) IHC staining of the cultured cells under phase contrast microscopy (upper panels), cytokeratin (middle panels) and vimentin (lower panels; magnification, x200). (B) Short-tandem repeat analyses of the two cell lines and the original PDX tumor. (C) Tumor growth curves (left panels) and images (right panels) of the tumors in response to treatment with vehicle or sorafenib. (D) Hematoxylin and eosin staining of original 004 PDX tumor (left panels), 004NA tumor (middle panels) and 004SR tumor (right panels; magnification, x100). (E) IHC using anti-CD34 antibody (left panels; magnification, x100), and blood vessel density by quantification of the percentage of $CD34^+$ pixels (right panel). $^{***}P<0.001$ by two-way analysis of variance. IHC, immunohistochemistry; 004 PDX, LIX-004 PDX; 004NA, LIXC-004NA; 004SR, LIXC-004SR; Sora, sorafenib; CD, cluster of differentiation.

Table I. *In vitro* inhibition of hepatocellular carcinoma tumor cell growth by different drug therapies.

	IC_{50}, μM					
Cell line	Sorafenib	Docetaxel	Doxorubicin	Vinblastine	5-FU	Erlotinib
LIXC-004NA	13.295	>20	0.675	<0.032	>200	13.998
LIXC-004SR	10.110	>20	>10	0.306	>200	>200

5-FU, fluorouracil; IC_{50}, half-maximal inhibitory concentration.

Activation of the sorafenib-resistant angiogenic pathway in the LIXC-004SR xenograft. IHC was performed to quantify the state of angiogenesis in the two tumor models (*in vivo* with or without sorafenib treatment). LIXC-004SR tumors that were not treated with sorafenib exhibited increased blood vessel density compared with the LIXC-004NA tumors (Fig. 2E), which may contribute to the faster tumor growth observed *in vivo*. Notably, in accordance with the tumor appearance, sorafenib significantly reduced blood vessel density in LIXC-004NA tumors, but not in LIXC-004SR tumors (Fig. 2E), indicating that an alternative angiogenic pathway may contribute to the sorafenib resistance in LIXC-004SR tumors.

Western blot analyses of the tumors indicated that sorafenib treatment induced similar changes in MEK, Akt and ERK phosphorylation in LIXC-004NA and LIXC-004SR tumors (data not shown), suggesting that the direct tumor cell inhibition or death may not contribute to the differences in sorafenib responses between these tumors. Microarray analyses were performed on the LIXC-004SR and LIXC-004NA cells. Among the differentially expressed genes, a group of genes involved in angiogenesis, including MMP-1, FGF5 and VEGFA, were upregulated in the LIXC-004SR cells when compared with expression in the LIXC-004NA cells (data not shown). This over-expression was confirmed by RT-qPCR analyses (Fig. 3A).

LIXC-004SR and LIXC-004NA culture supernatant was used in further analyses, as soluble factors mediate tumor-host communication *in vivo*. LIXC-004SR, but not LIXC-004NA, culture supernatant was able to significantly induce HUVEC proliferation (Fig. 3B), and induce Akt and ERK phosphorylation in HUVECs (Fig. 3C), suggesting that pro-angiogenic factors were present in the LIXC-004SR culture supernatant. This HUVEC Akt and ERK phosphorylation was only inhibited by the combination of sorafenib and an FGFR1 selective inhibitor, AZD4547 almost completely (Fig. 3D). These data suggest that LIXC-004SR cells were able to induce endothelial cell signaling and proliferation that was insensitive to sorafenib treatment. The FGF pathway may be one of the mechanisms involved.

To examine whether or not the FGF pathway serves a role in tumor growth *in vivo*, LIXC-004SR tumor-bearing mice were treated with vehicle, sorafenib, AZD4547, or the combination of sorafenib and AZD4547. The LIXC-004SR tumors were resistant to sorafenib treatment. The tumor growth was inhibited by AZD4547 and was not further inhibited by the addition of sorafenib (Fig. 3E). The results suggest that the FGF pathway contributed towards LIXC-004SR tumor growth *in vivo*.

LIXC-004SR cells display genome instability. Whole exome sequencing and RNA sequencing analyses of the cell lines were performed and compared with the whole genome sequencing data from the LIX-004 PDX tumor. It was revealed that >98.5% of the single nucleotide polymorphisms (SNPs) observed in the two cell lines were present in the LIX-004 PDX tumor (Fig. 4A), demonstrating that the cell lines effectively preserved the genetic mutations of the PDX model. Notably, 123 SNPs were revealed to be unique to LIX-004SR cells compared with the 33 unique SNPs observed in the LIX-004NA cells.

To investigate the potential source of this acquired drug resistance, chromosomal analyses were performed, as genome instability was suggested to be an enabling Hallmark of Cancer (15). LIXC-004NA cells exhibited a peak of 55±4 chromosomes with ~50% of the cells exhibiting a chromosome number within this range (Fig. 4B). This number is close to the normal human chromosomal number of 46. LIXC-004SR cells, on the other hand, presented with a more diverse distribution of chromosomal numbers with a peak at 85±4 chromosomes and with only ~25% of the cells within the range (Fig. 4B). These data suggest that genome instability may be associated with the tumor size increase observed following long-term sorafenib treatment.

Discussion

At present, sorafenib is the only approved targeted therapy for liver cancer (5). However, acquired sorafenib resistance has prevented patients from experiencing the long-term benefits of this drug. A number of drug resistance studies have focused on tumor cell lines either naturally resistant or induced to become resistant in tissue culture. Such 'tumor-centric' approaches have led to 'tumor-centric' mechanisms of drug resistance (16). However, these types of approaches do not take into account the role served by tumor-host interaction. In previous studies, tumor microenvironment/tumor stroma has been revealed to contribute toward tumor drug resistance (17,18). The present study used *in vivo* PDX models to recapitulate the process of drug resistance *in vivo*, since PDX models are able to preserve a number of the characteristics of clinical tumor samples and the drug response is more strongly associated with clinical drug efficacy when compared with conventional cell line-derived xenograft models (19). One

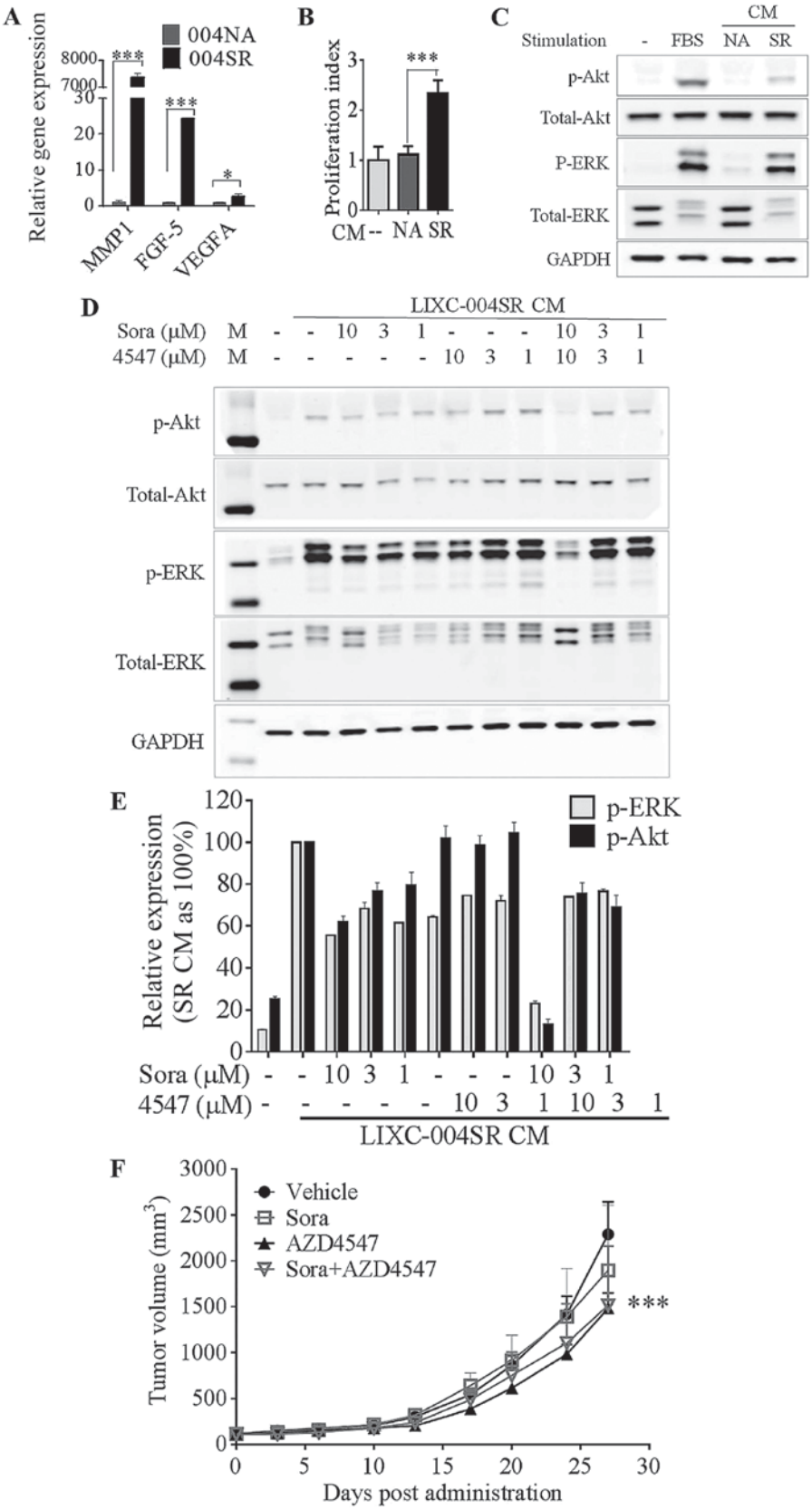

Figure 3. LIXC-004SR activates an alternative angiogenic pathway. (A) Reverse transcription-quantitative polymerase chain reaction analyses of selected differentially expressed genes; MMP-1, FGF-5 and VEGF-A. *P<0.05, ***P<0.0001; two-way ANOVA with Bonferroni post tests. (B) HUVEC proliferation. ***P<0.001, one-way ANOVA. (C) HUVEC Akt and ERK phosphorylation determination by western blot analysis. (D) Western blot analyses of 004SR supernatant-induced HUVEC Akt and ERK phosphorylation in the presence of sorafenib and AZD4547 (upper panel) and quantification of the western blot analyses (lower panel, data represent two separate experiments). (E) 004SR tumor-bearing mice were treated with vehicle, sorafenib, AZD4547, or the combination of AZD4547 and sorafenib. (F) AZD4547 inhibited tumor progression (***P<0.001 vs. the vehicle control group on day 27; two-way ANOVA with Bonferroni post hoc tests). The study was repeated once with similar results. 004SR, LIXC-004SR; MMP-1, matrix metalloproteinase 1; FGF-5, fibroblast growth factor 5; VEGF-A, vascular endothelial growth factor A; ANOVA, analysis of variance; HUVEC, human umbilical vein endothelial cells; ERK, extracellular-signal-regulated kinase; CM, conditioned medium.

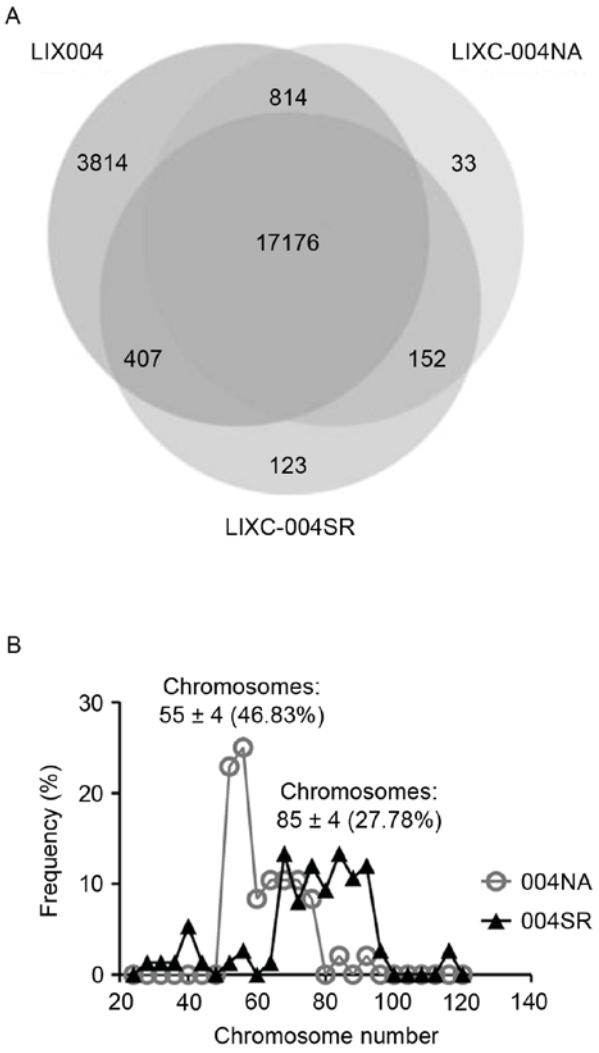

Figure 4. Genetic analyses of 004NA and 004SR cells. (A) Single nucleotide polymorphism analysis was performed by comparing whole exome sequencing of the cell lines and whole genome sequencing data from LIX004. (B) Quantification of chromosome number distribution in chromosomal analyses of 004NA and 004SR cell lines. The numbers in the parentheses following the chromosome number range represent the percentage of cells whose chromosome numbers are within this range. 004NA, LIXC-004NA; 004SR, LIXC-004SR; LIX004, the parental PDX model.

of the drawbacks of the model used in the present study is that it requires the use of immune-compromised animals, namely Nu/Nu mice. These animals lack functional T cells and thus, do not account for the mechanisms that these cells are involved in. However, these animals have a number of the components of the tumor microenvironment, including endothelial cells, fibroblasts, pericytes, myeloid cells, B cells and the extracellular matrix (19). In addition, certain key factors in tumor-host interactions, including VEGF and granulocyte-colony stimulating factor, may induce similar signals through receptors in mice. Therefore, despite the lack of T cells, PDX models possess several aspects of relevant tumor-host interactions.

Another drawback of the system used in the present study is that the tumor was implanted subcutaneously, instead of orthotopically in the liver. This may lead to loss of the tumor organ-microenvironment. By contrast, one of the key advantages of PDX models is that the tumor is maintained *in vivo* and it carries sufficient structural information to ensure its normal growth behavior (19). In the present study, adenocarcinomas formed gland-like structures despite having been implanted subcutaneously and even did so following several rounds of *in vivo* passaging (20). Furthermore, the pathological diagnosis of these tumors was poorly differentiated HCC, as was the original clinical diagnosis, indicating the preservation of at least some of the clinical characteristics of the human tumor sample. In the present study, the resistance of LIXC-004SR to sorafenib developed in the presence of tumor-host interaction, making it a more relevant model for drug resistance research.

In the present study, the FGF pathway is suggested to be involved in acquired sorafenib resistance. This finding is infrequently reported in 'tumor-centric' sorafenib-resistance studies (21-24). However, this novel finding appears to be reasonable, as the FGF pathway has been reported to be one of the most dysregulated pathways in patients with HCC (6,25). FGF5 has been reported to be upregulated in pancreatic cancer patient samples and to contribute to the malignant phenotype (16,26-28). A more recent study revealed an association between FGF5 and a more aggressive HCC phenotype, and suggested FGF5 as an oncogene in HCC, and thus its potential as a novel therapeutic target for HCC (29). Tovar *et al* (30) also revealed that FGF signaling contributed toward sorafenib resistance in cell line-derived HCC xenografts following sorafenib treatment *in vivo*.

In the present study, LIXC-004SR cells also demonstrated signs of genome instability when compared with the LIXC-004NA cells. As genome instability is an enabling Hallmark of Cancer (15), it may contribute to the acquired *in vivo* sorafenib resistance. Given the heterogeneity of human cancer, particularly liver cancer, and the chromosome instability observed in the present study, this type of study is unlikely to cover all the potential mechanisms of acquired drug resistance. The fact that the FGFR1 inhibitor only resulted in a certain degree of inhibition of LIXC-004SR xenograft tumor growth *in vivo* suggests that additional mechanism(s) exist in this model.

Overall, the approach of the present study has produced a relevant animal model of acquired sorafenib resistance from a PDX model. From this *in vivo* model, the alternative angiogenic pathways and genome instability, which were previously overlooked in drug resistance studies focusing only on tumor cells in tissue culture, were rediscovered. The model also exhibited characteristics of multi-drug resistance. The generation of a sister cell line, with an identical genetic background and only differing in drug sensitivity, makes this pair of cell lines and associated xenograft and PDX models valuable tools in the study of drug resistance. The understanding and further utilization of this model system may facilitate research and drug development regarding the prevention and treatment of drug resistance, and will hopefully contribute toward sustained therapeutic efficacy and long-term survival in cancer patients.

Acknowledgements

The present study was supported by the Shanghai Municipal Commission of Science and Technology (grant no. 14DZ2252000), the National Natural Science Foundation

of China (grant no. 81274146), the 333 High Level Project of Jiangsu Province (grant no. BRA2014245) and Funding for Priority Academic Program Development of Jiangsu Higher Education Institution (PAPD). The authors would also like to thank Dr Charles Yang (Department of Biology, Shanghai ChemPartner Co. Ltd.) for providing editorial assistance and advice.

References

1. Jemal A, Bray F, Center MM, Ferlay J, Ward E and Forman D: Global cancer statistics. CA Cancer J Clin 61: 69-90, 2011.
2. Liu L, Cao Y, Chen C, Zhang X, McNabola A, Wilkie D, Wilhelm S, Lynch M and Carter C: Sorafenib blocks the RAF/MEK/ERK pathway, inhibits tumor angiogenesis, and induces tumor cell apoptosis in hepatocellular carcinoma model PLC/PRF/5. Cancer research 66: 11851-11858, 2006.
3. Llovet JM, Ricci S, Mazzaferro V, Hilgard P, Gane E, Blanc JF, de Oliveira AC, Santoro A, Raoul JL, Forner A, *et al*: Sorafenib in advanced hepatocellular carcinoma. N Engl J Med 359: 378-390, 2008.
4. Abou-Alfa GK, Schwartz L, Ricci S, Amadori D, Santoro A, Figer A, De Greve J, Douillard JY, Lathia C, Schwartz B, *et al*: Phase II study of sorafenib in patients with advanced hepatocellular carcinoma. J Clin Oncol 24: 4293-4300, 2006.
5. Cheng AL, Kang YK, Chen Z, Tsao CJ, Qin S, Kim JS, Luo R, Feng J, Ye S, Yang TS, *et al*: Efficacy and safety of sorafenib in patients in the Asia-Pacific region with advanced hepatocellular carcinoma: A phase III randomized, double-blind, placebo-controlled trial. Lancet 10: 25-34, 2009.
6. Moeini A, Cornellà H and Villanueva A: Emerging signaling pathways in hepatocellular carcinoma. Liver Cancer 1: 83-93, 2012.
7. Santoro A, Rimassa L, Borbath I, Daniele B, Salvagni S, Van Laethem JL, Van Vlierberghe H, Trojan J, Kolligs FT, Weiss A, *et al*: Tivantinib for second-line treatment of advanced hepatocellular carcinoma: A randomised, placebo-controlled phase 2 study. Lancet Oncol 14: 55-63, 2013.
8. Villarroel MC, Rajeshkumar NV, Garrido-Laguna I, De Jesus-Acosta A, Jones S, Maitra A, Hruban RH, Eshleman JR, Klein A, Laheru D, *et al*: Personalizing cancer treatment in the age of global genomic analyses: PALB2 gene mutations and the response to DNA damaging agents in pancreatic cancer. Mol Cancer Ther 10: 3-8, 2011.
9. Hidalgo M, Bruckheimer E, Rajeshkumar NV, Garrido-Laguna I, De Oliveira E, Rubio-Viqueira B, Strawn S, Wick MJ, Martell J and Sidransky D: A pilot clinical study of treatment guided by personalized tumorgrafts in patients with advanced cancer. Mol Cancer Ther 10: 1311-1316, 2011.
10. Das Thakur M, Salangsang F, Landman AS, Sellers WR, Pryer NK, Levesque MP, Dummer R, McMahon M and Stuart DD: Modelling vemurafenib resistance in melanoma reveals a strategy to forestall drug resistance. Nature 494: 251-255, 2013.
11. Wilhelm SM, Carter C, Tang L, Wilkie D, McNabola A, Rong H, Chen C, Zhang X, Vincent P, McHugh M, *et al*: BAY 43-9006 exhibits broad spectrum oral antitumor activity and targets the RAF/MEK/ERK pathway and receptor tyrosine kinases involved in tumor progression and angiogenesis. Cancer Res 64: 7099-7109, 2004.
12. Gavine PR, Mooney L, Kilgour E, Thomas AP, Al-Kadhimi K, Beck S, Rooney C, Coleman T, Baker D, Mellor MJ, *et al*: AZD4547: An orally bioavailable, potent, and selective inhibitor of the fibroblast growth factor receptor tyrosine kinase family. Cancer Res 72: 2045-2056, 2012.
13. Xin H, Wang K, Hu G, Xie F, Ouyang K, Tang X, Wang M, Wen D, Zhu Y and Qin X: Establishment and characterization of 7 novel hepatocellular carcinoma cell lines from patient-derived tumor xenografts. PLoS One 9: e85308, 2014.
14. Livak KJ and Schmittgen TD: Analysis of relative gene expression data using real-time quantitative PCR and the 2(-Delta Delta C(T)) method. Methods 25: 402-408, 2001.
15. Hanahan D and Weinberg RA: Hallmarks of cancer: The next generation. Cell 144: 646-674, 2011.
16. Zhai B and Sun XY: Mechanisms of resistance to sorafenib and the corresponding strategies in hepatocellular carcinoma. World J Hepatol 5: 345-352, 2013.
17. Olive KP, Jacobetz MA, Davidson CJ, Gopinathan A, McIntyre D, Honess D, Madhu B, Goldgraben MA, Caldwell ME, Allard D, *et al*: Inhibition of Hedgehog signaling enhances delivery of chemotherapy in a mouse model of pancreatic cancer. Science 324: 1457-1461, 2009.
18. Sebens S and Schafer H: The tumor stroma as mediator of drug resistance-a potential target to improve cancer therapy? Curr Pharm Biotechnol 13: 2259-2272, 2012.
19. Sausville EA and Burger AM: Contributions of human tumor xenografts to anticancer drug development. Cancer Res 66: 3351-3354, 2006.
20. Hu G, Li F, Ouyang K, Xie F, Tang X, Wang K, Han S, Jiang Z, Zhu M, Wen D, *et al*: Intrinsic gemcitabine resistance in a novel pancreatic cancer cell line is associated with cancer stem cell-like phenotype. Int J Oncol 40: 798-806, 2012.
21. Chen KF, Chen HL, Tai WT, Feng WC, Hsu CH, Chen PJ and Cheng AL: Activation of phosphatidylinositol 3-kinase/Akt signaling pathway mediates acquired resistance to sorafenib in hepatocellular carcinoma cells. J Pharmacol Exp Ther 337: 155-161, 2011.
22. Serova M, de Gramont A, Tijeras-Raballand A, Dos Santos C, Riveiro ME, Slimane K, Faivre S and Raymond E: Benchmarking effects of mTOR, PI3K, and dual PI3K/mTOR inhibitors in hepatocellular and renal cell carcinoma models developing resistance to sunitinib and sorafenib. Cancer Chemother Pharmacol 71: 1297-1307, 2013.
23. Tai WT, Cheng AL, Shiau CW, Liu CY, Ko CH, Lin MW, Chen PJ and Chen KF: Dovitinib induces apoptosis and overcomes sorafenib resistance in hepatocellular carcinoma through SHP-1-mediated inhibition of STAT3. Mol Cancer Ther 11: 452-463, 2012.
24. van Malenstein H, Dekervel J, Verslype C, Van Cutsem E, Windmolders P, Nevens F and van Pelt J: Long-term exposure to sorafenib of liver cancer cells induces resistance with epithelial-to-mesenchymal transition, increased invasion and risk of rebound growth. Cancer Lett 329: 74-83, 2013.
25. Sawey ET, Chanrion M, Cai C, Wu G, Zhang J, Zender L, Zhao A, Busuttil RW, Yee H, Stein L, *et al*: Identification of a therapeutic strategy targeting amplified FGF19 in liver cancer by Oncogenomic screening. Cancer Cell 19: 347-358, 2011.
26. Kornmann M, Ishiwata T, Beger HG and Korc M: Fibroblast growth factor-5 stimulates mitogenic signaling and is overexpressed in human pancreatic cancer: Evidence for autocrine and paracrine actions. Oncogene 15: 1417-1424, 1997.
27. Tian X, Chen G, Zhou S, Henne-Bruns D, Bachem M and Kornmann M: Interactions of pancreatic cancer and stellate cells are mediated by FGFR1-III isoform expression. Hepatogastroenterology 59: 1604-1608, 2012.
28. Allerstorfer S, Sonvilla G, Fischer H, Spiegl-Kreinecker S, Gauglhofer C, Setinek U, Czech T, Marosi C, Buchroithner J, Pichler J, *et al*: FGF5 as an oncogenic factor in human glioblastoma multiforme: Autocrine and paracrine activities. Oncogene 27: 4180-4190, 2008.
29. Fang F, Chang RM, Yu L, Lei X, Xiao S, Yang H and Yang LY: MicroRNA-188-5p suppresses tumor cell proliferation and metastasis by directly targeting FGF5 in hepatocellular carcinoma. J Hepatol 63: 874-885, 2015.
30. Tovar V, Cornella H, Moeini A, Vidal S, Hoshida Y, Sia D, Peix J, Cabellos L, Alsinet C, Torrecilla S, *et al*: Tumour initiating cells and IGF/FGF signalling contribute to sorafenib resistance in hepatocellular carcinoma. Gut 66: 530-540, 2017.